Major flood event in the Mullerthal region on 1 June 2018: event analysis and predictability

Luca Mathias*

*M.Sc. Meteorologist, MeteoLux, Administration de la Navigation Aérienne

Email: luca.mathias@airport.etat.lu

First published: 31 May 2019 / Last modified: 31 May 2019

1. Introduction

During the early hours of 1 June 2018, the Mullerthal region in the middle eastern part of Luxembourg (cf. Fig. 1) was hit by heavy convective rainfall that triggered catastrophic flash floods. The Mullerthal region is dominated by a north-south orientated river valley, surrounded by a hilly landscape with altitudes up to 420 m and steep slopes (Fig. 1). The river Black Ernz (fr. *Ernz Noire*) flows through Mullerthal and is linked to many smaller watercourses (Fig. 1). Severe bank erosions and landslides occurred locally, not only in the Mullerthal region but also north of it between Beaufort and Echternach[1]. Hence, a hotel and a camping site located in Mullerthal were substantially damaged. Three weeks after the event, a first estimate of total losses amounting to roughly 5 million euros was reported.

The purpose of this study is to analyse the synoptic- to mesoscale characteristics and the predictability of this extreme weather event. Remote sensing measurements, weather station observations, as well as numerical weather prediction (NWP) model data, enable a detailed examination. This article is structured as follows. Section 2 describes the data used in this study and an overview of the synoptic-scale situation will be provided in section 3. A radar and satellite analysis of the flood event is given in section 4 and the precipitation observations are examined in section 5. The predictability of this event will be discussed in section 6. The last section includes a short summary and the conclusions.

1 https://gouvernement.lu/fr/actualites/toutes_actualites/communiques/2018/06-juin/12-bausch-kersch-mullerthal.html

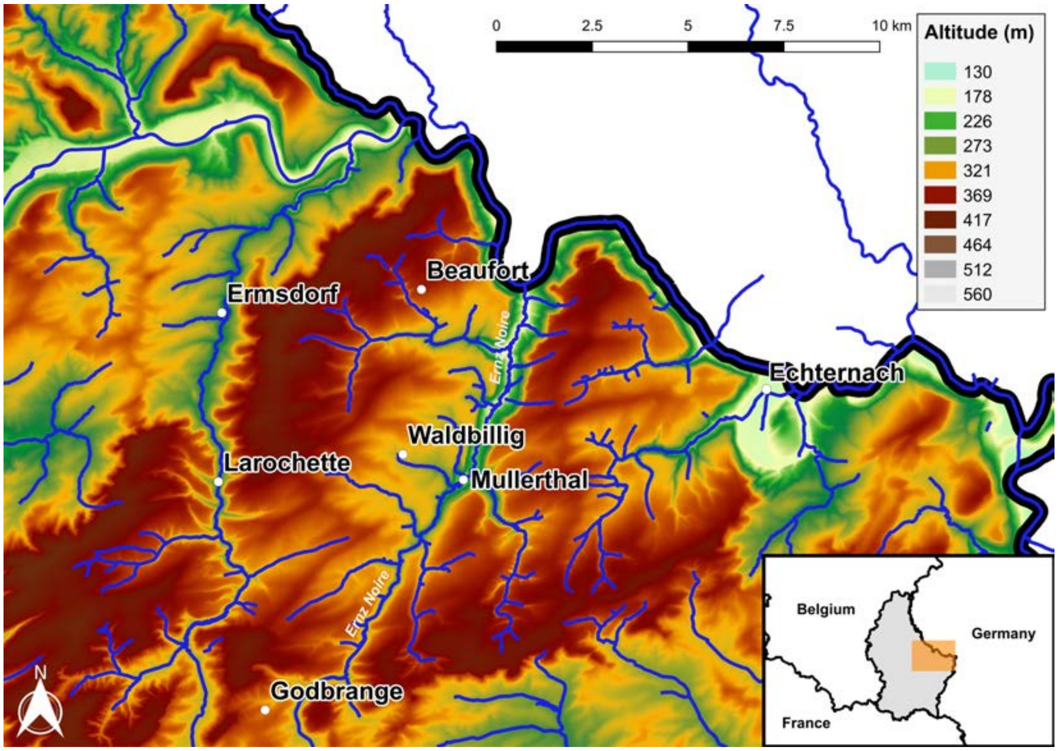

Figure 1: Topographic map of the investigation area in Luxembourg (shaded orange in the inset on the bottom-right-hand side). The watercourses are denoted by dark blues lines.

2. Data

The in situ measurements of precipitation and wind include data from the automated surface weather station network operated by the meteorological department of the Administration des Services Techniques de l'Agriculture (ASTA). The data has a temporal resolution of 10 minutes. Data from the operational C-band radar in Wideumont operated by the Royal Meteorological Institute of Belgium (RMIB) is used to document the mesoscale evolution of the convection. The Doppler radar performs a multiple elevation scan every 5 minutes with a beam width of one degree and a horizontal resolution of 250 m in range. Reflectivity-only elevation scans have a maximum range of 250 km, whereas combined reflectivity-velocity elevation scans have a smaller maximum coverage of 125 km. The radar data is processed and visualized using the open source software NLradar created by Bram van't Veen from the University of Utrecht. Data from the radar-based quantitative precipitation estimation method Radar-Online-Aneichung (RADOLAN) developed by the German Weather Service

(Deutscher Wetterdienst; DWD) will be analysed as well. The RADOLAN composite has a grid length of 1 km (Bartels et al. 2004).

In addition to the in situ and radar data, ERA5 reanalysis data from the European Centre for Medium-Range Weather Forecasts (ECMWF) will be used to examine the synoptic-scale conditions. ERA5 was produced using 4D-Var data assimilation with the model cycle 41r2 of ECMWF's Integrated Forecast System (IFS). The hourly reanalysis data output has a native horizontal grid spacing of 31 km and 137 levels in the vertical (Hersbach et al. 2019). Furthermore, the predictability will be discussed using the convection-resolving limited-area NWP model Applications de la Recherche à l'Opérationnel à Mésoéchelle (AROME; Seity et al. 2011) operated by Météo-France and operationally used by MeteoLux. AROME has a native horizontal grid interval of 1.3 km and 90 vertical levels. The initial and lateral boundary conditions for AROME are provided by the global NWP model Action de Recherche Petite Echelle Grande Echelle (ARPEGE; Courtier et al. 1991) which is also operated by Météo-France. The operational ECMWF's ensemble prediction system (EPS) is also considered. ECMWF-EPS is based on the IFS cycle 43r3 and it consists of 50 perturbed members and one control run with a native horizontal grid spacing of 18 km and 91 levels in the vertical. In contrast to AROME, deep moist convection (DMC) is parameterised in the IFS model. The convection scheme is based on the bulk mass-flux approach after Tiedtke (1989), which has been enhanced by Bechtold et al. (2014).

3. Synoptic-scale atmospheric conditions

On 31 May 2018, a meridional flow was active in the middle to upper troposphere over Western Europe, which was mainly controlled by an ill-defined and weakening omega ridge centred over Eastern Europe. At 2100 UTC, a negatively tilted trough extended from the English Channel to northwestern Italy (Fig. 2a), splitting the meridional mid-level flow into a southwesterly component over the western Mediterranean and a southeasterly component over Benelux and western Germany. A filament of enhanced cyclonic vorticity was diagnosed along the axis of this upper-air trough (Fig. 2a). An upper-tropospheric vorticity maximum was situated over the Western Alps (Fig. 2a), which moved slowly to northern France until 1 June 2018 1200 UTC. Weak differential cyclonic vorticity advection occurred downstream of this vorticity maximum, and thus caused large-scale forced upward motion. Furthermore, a weak jet streak was present at the poleward flank of the trough over northern France (cf. Fig. 2a with 2b).

The low-level conditions were characterised by a weak pressure gradient over large parts of Europe, with an area of relatively low pressure extending from the British Isles over Germany to Southeastern Europe (Fig. 2c). This area was covered by a subtropical air mass with 850 hPa temperatures ranging from 10 to 15 °C (not shown). Moreover, high amounts of tropospheric water vapour were detected in the regime of the warm air mass over northern France, Benelux and Germany, with precipitable water (PWAT) contents of 25 to 35 mm (Fig. 2c). An area-averaged vertical profile of the eastern part of the Greater Region indicated a mean mixing ratio of about 10 g kg^{-1} in the lowest 50 to 100 hPa (Fig. 2d). The combination of the enhanced boundary layer moisture and a conditionally unstable lapse rate profile resulted in a most-unstable convective available potential energy (CAPE) of about 1000 J kg^{-1} and a most-unstable convective inhibition (CIN) of -45 J kg^{-1} (Fig. 2d). The most-unstable air parcel corresponds to an air parcel near the surface in this case. However, since a thin layer of stable air was present near the surface due to the arising nocturnal cooling (Fig. 2d), an air parcel located above this layer at about 925 hPa was more likely to reach the level of free convection because of lower CIN (~ -25 J kg^{-1}), though having less CAPE (~ 500 J kg^{-1}).
Additionally, the lower-tropospheric air flow was decoupled from the mid- to upper-tropospheric flow. Weak westerly to northwesterly winds (≤ 6 m s^{-1}) were dominant below 700 hPa, whereas south-easterly winds prevailed from 700 hPa upwards to the tropopause (Fig. 2d). Hence, the vertical wind speed shear within the lowest 3 km of the troposphere was very weak, but the speed shear between approximately 3.6 and 11 km altitude (650 to 225 hPa) was significantly stronger with about 20 m s^{-1} (Fig. 2d).

In brief, the synoptic-scale environment was favourable for the development of DMC. A rich boundary layer moisture and conditionally unstable lower- to mid-tropospheric lapse rates resulted in moderate latent instability. The forcing to initiate DMC storms was mainly provided by sub-synoptic-scale processes (e.g., low-level convergence zones, outflow boundaries, forced orographic ascent). The weak synoptic-scale lift occurring downstream of the trough may have been important for conditioning the large-scale environment for DMC and for supporting elevated DMC.

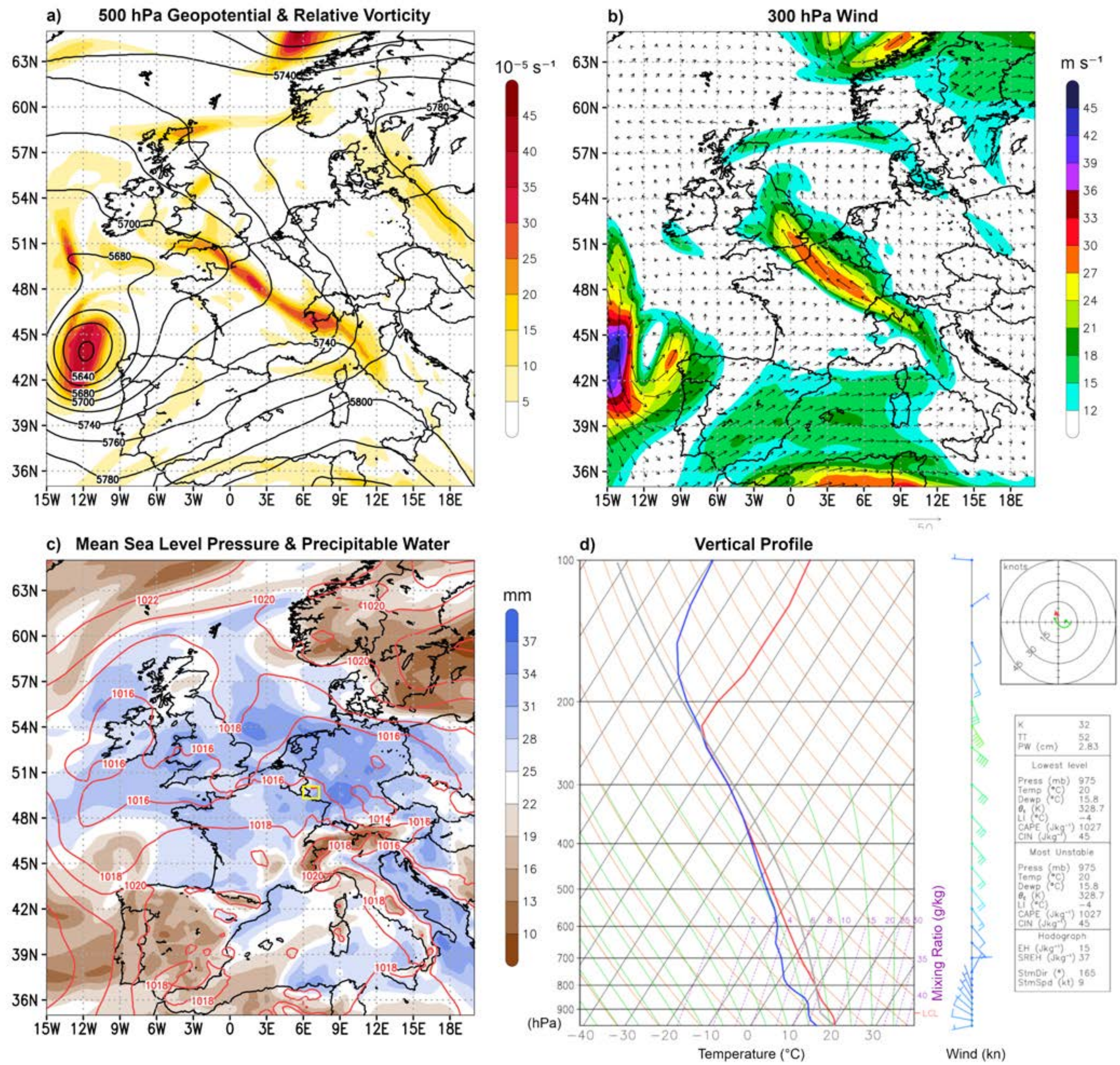

Figure 2: ERA5 reanalysis of the synoptic-scale conditions on 31 May 2018 at 2100 UTC over Western Europe. (a) 500 hPa geopotential height (black lines; gpm) and maximum cyclonic relative vorticity (10^{-5} s^{-1}) between 500 and 300 hPa. (b) 300 hPa wind speed and vector direction (m s^{-1}). (c) Mean sea level pressure (red lines; hPa) and total column water vapour/precipitable water (mm). (d) Skew-T log-p diagram of an area-averaged vertical profile (area is denoted by the yellow box in (c)). The red (blue) curve represents the temperature (dew point) and the grey curve represents the ascent trajectory of the most unstable parcel.

4. Mesoscale analysis

At the beginning of the night from 31 May to 1 June 2018, strong DMC was active over southern Germany. At 2000 UTC, a mesoscale convective system (MCS) was situated over southeastern Germany (feature “1” in Fig. 3a), which originated from the consolidation of scattered thunderstorms having been initiated in the afternoon. A second MCS started to form over southwestern Germany near the Swiss border (feature “2” in Fig. 3a). As the eastern MCS weakened progressively until 2200 UTC, its remnants merged with the strengthening and northwestward moving MCS over southwestern Germany. Consequently, a major MCS had developed by 0000 UTC on 1 June with minimum cloud top temperatures between -70 and -65 °C (Fig. 3b). The moderate mid- to upper-tropospheric vertical wind shear downstream of the trough located over Switzerland may have supported the organisation of this MCS (cf. Coniglio et al. 2006, Chen et al. 2015). Since the shear in the lower troposphere was very weak, the MCS struggled to maintain linearly-organized convection at its leading edge. Hence, excessive precipitation and local-scale flooding were the main threats due to reduced storm motion.

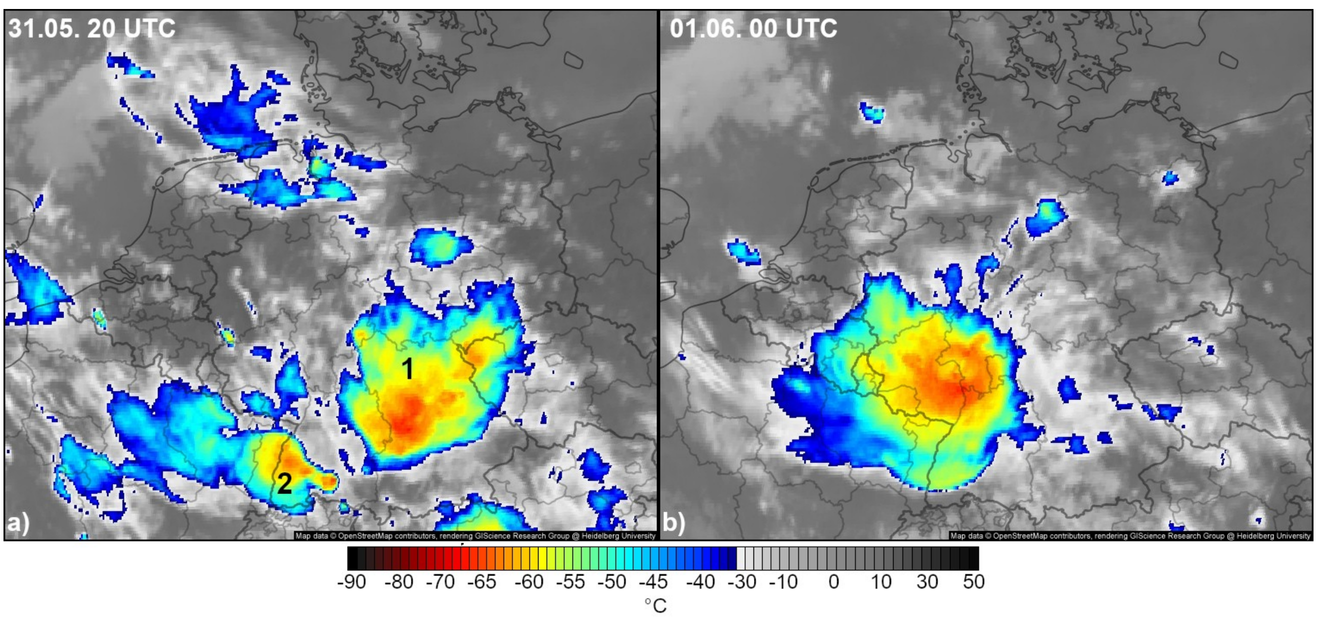

Figure 3: Meteosat colour-enhanced infrared (IR) 10.8 µm channel images with brightness temperature of cloud tops for (a) 31.05.2018 2000 UTC and (b) 01.06.2018 0000 UTC. The features “1” and “2” in (a) are quoted in the text. Source: https://kachelmannwetter.com/de/sat/top-alarm-15min.html

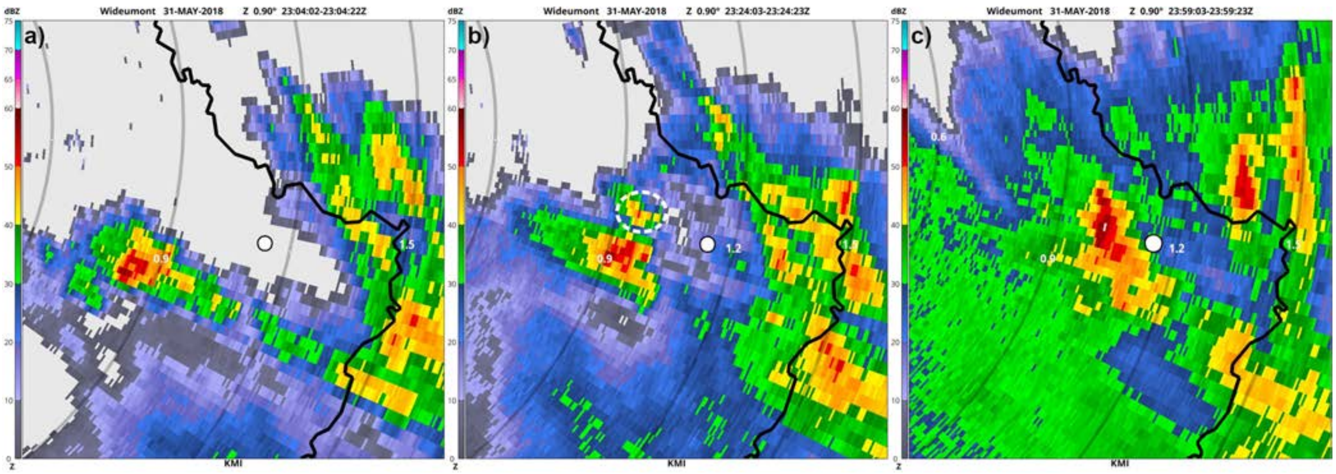

Figure 4: 0.9° base reflectivity (dBZ) measured by the RMIB radar in Wideumont at (a) 2304 UTC, (b) 2324 UTC, and (c) 2359 UTC on 31 May 2018. The grey concentric circles indicate the height (km) of the radar beam. The white dot denotes the location of Mullerthal.

While the MCS approached the Greater Region from the southeast, a few shallow convective cells formed over southern Luxembourg as of 2200 UTC, which dissipated until 2245 UTC. However, at 2300 UTC, a strong convective cell was initiated over Mersch to the west of the Mullerthal region (Fig. 4a). This cell then slowly moved eastward and merged with a small feeder cell (denoted by a white dashed -line ellipse in Fig. 4b) while reaching Larochette at around 2330 UTC (Fig. 4b). At the same time, the cell started to produce lightning (not shown). Subsequently, the storm got embedded into the large-scale precipitation field of the northwestward moving MCS (cf. Fig. 4a with 4b) and it further intensified. At 0000 UTC on 1 June, the embedded storm was situated over the elevation between Mullerthal and Ermsdorf (cf. Fig. 1) with a local low-level reflectivity maximum of 60 dBZ (Fig. 4c). Furthermore, the convective cell possessed a vertically stacked reflectivity core with values above 40 dBZ reaching an altitude of about 8 km (not shown). The intense precipitation core remained quasi-stationary over the aforementioned area between Mullerthal and Ermsdorf until 0030 UTC (Figs. 5a,b). At the ASTA weather station in Waldbillig, heavy rainfall began at about 0000 UTC, accompanied by a convective wind gust of 70 km h^{-1} (Fig. 6b).

Concurrently, strong DMC embedded in the MCS (denoted by a white dashed-line ellipse in Fig. 5a) approached the Mullerthal region from the east. This convective segment gradually merged with the quasi-stationary cell (cf. Figs 5a,b with Fig. 5c), such that the strongest convective rainfall got slightly displaced to the north of Mullerthal (Figs 5c,d). Overall, low-level reflectivity values of 45 to 55 dBZ were present from 0000 to 0100 UTC over the elevated area between Ermsdorf and Mullerthal, and from 0050 to 0105 UTC near the confluence zone of the two rivers Black Ernz and Sûre to the east of Beaufort (cf. Fig.1 with Figs. 4 and 5). After 0115 UTC, the precipitation rate weakened significantly over both above-mentioned areas, as the MCS slowly crossed the Grand-Duchy and moved to Belgium (not shown). Light rain continued to fall over the Mullerthal region until the early morning of 1 June 2018 (see Fig. 6b).

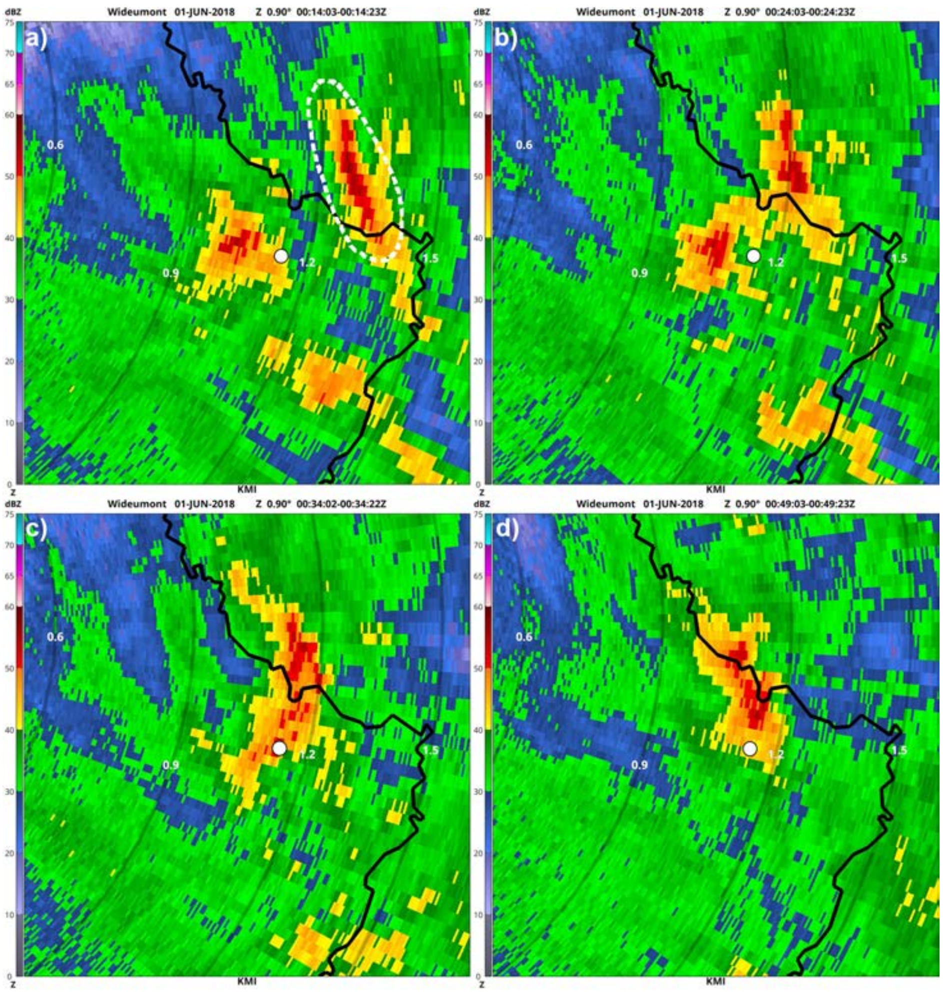

Figure 5: 0.9° base reflectivity (dBZ) measured by the RMIB radar in Wideumont at (a) 0014 UTC, (b) 0024 UTC, (c) 0034 UTC, and (d) 0049 UTC on 01 June 2018. The grey concentric circles indicate the height (km) of the radar beam. The white dot denotes the location of Mullerthal.

5. Observed precipitation

As already shown in section 4, relatively long-lasting and intense precipitation rates caused the extreme rainfall amounts near Mullerthal. The RADOLAN precipitation estimates indicated an hourly accumulation of 20 to 50 mm within a broader area between Ermsdorf and Mullerthal slightly west of the Black Ernz for the time period 31 May 2350 UTC – 01 June 0050 UTC, with two peak pixel values of 52.3 and 52.2 mm near Waldbillig (Fig. 6a). However, when comparing the RADOLAN pixel values with in situ precipitation data, it is likely that RADOLAN underestimated the rainfall within the aforementioned area (see Fig. 6a). For instance, the ASTA weather station in Waldbillig measured an hourly precipitation amount of 69.4 mm (Fig. 6). This in situ value is supported by a private semi-professional weather station located in Christnach (roughly 1 km southwest of Waldbillig), which registered 73.2 mm of rain between 2345 and 0045 UTC. A similar underestimation by RADOLAN for heavy convective rainfall was also observed for the flood event in the Vallée de l'Ernz on 22 July 2016 (Pfister et al. 2018, Mathias 2019). Nonetheless, the rainfall measurements at the three surrounding ASTA weather stations in Bettendorf, Echternach, and Godbrange matched well with the RADOLAN values (Fig. 6a). When considering a 6 hour accumulation period (1 June 0000 UTC to 0600 UTC), a precipitation amount of 100.6 mm was measured in Waldbillig and 53.8 mm fell at the Airport Luxembourg-Findel. Furthermore, measurements from the supplementary station network operated by the Kachelmann Group revealed 6-hourly accumulated precipitation of 80.1 mm in Wasserbillig and 60.7 mm in Stolzembourg[2].

Altogether, it can be estimated that precipitation amounts of 65 to 80 mm accumulated within one hour over the elevated area between Ermsdorf and Mullerthal (cf. Fig. 1 with Fig. 6a), which corresponds to the climatological monthly mean value for that region during summer. Thus, the excessive precipitation occurred primarily over the tributaries Kaasselbaach and Bëllegerbaach near Waldbillig, which flow into the Black Ernz in the Mullerthal (Fig. 6a). This hydrological process was likely crucial for triggering the flash floods and landslides. Other hydrological ingredients are not going to been dealt with in this study, but include such topics as soil moisture, surface runoff, infiltration rate, and land use.

2 https://kachelmannwetter.com/de/messwerte/luxemburg/niederschlagssumme-12h/20180601-0600z.html

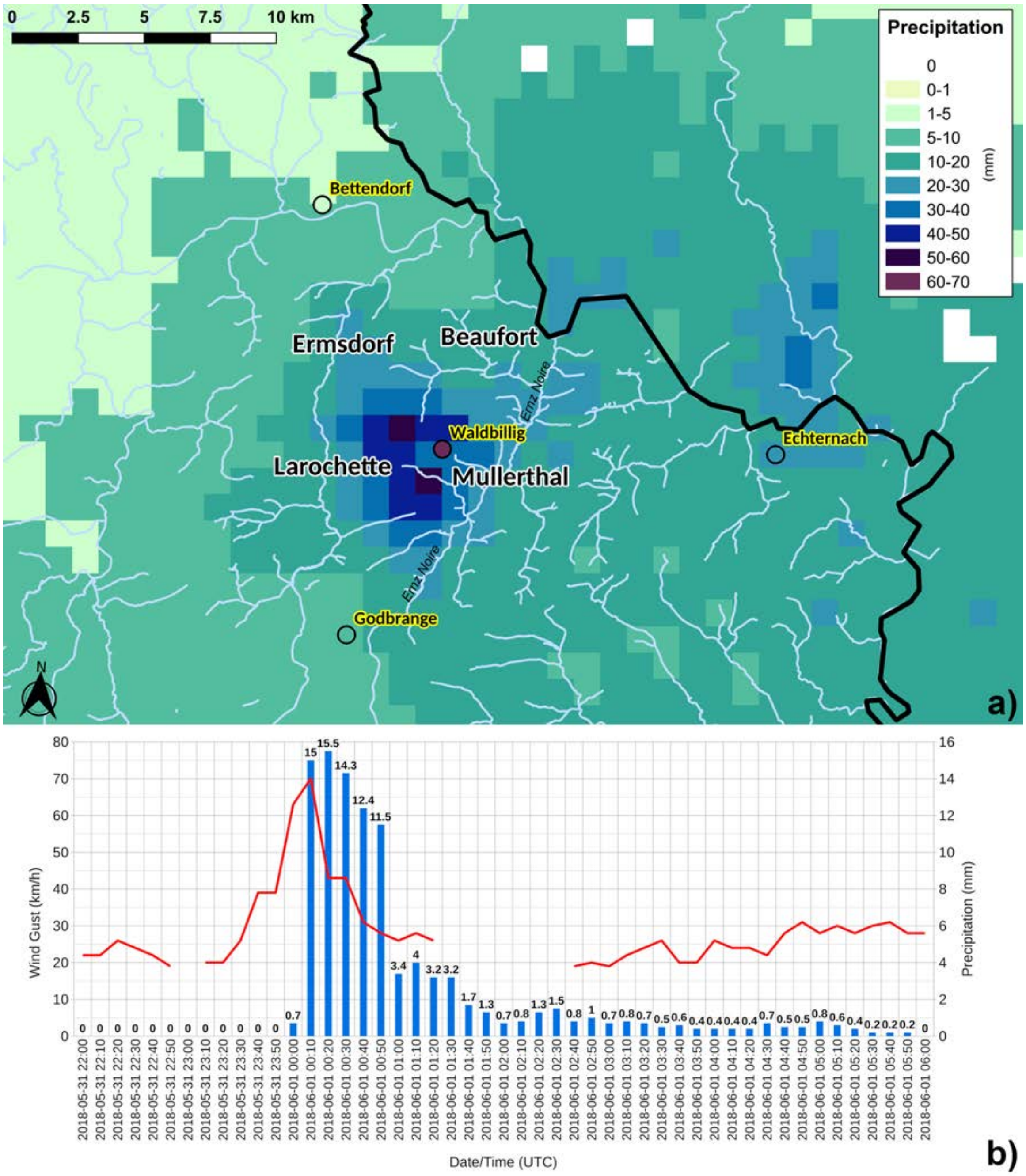

Figure 6: (a) Accumulated precipitation between 2350 UTC on 31 May 2018 and 0050 UTC on 01 June 2018 in the study area, derived by RADOLAN (shaded; mm) and measured by ASTA surface weather stations (towns with yellow text buffer; Waldbillig: 69.4 mm, Echternach: 25.5 mm, Godbrange: 7.8 mm, Bettendorf: 2.2 mm). (b) Accumulated precipitation (blue bars; mm) and maximum wind gusts (red line; km h^{-1}) during the preceding 10 minutes measured by the ASTA surface weather station in Waldbillig between 2200 UTC on 31 May 2018 and 0600 UTC on 1 June 2018.

6. Predictability

Five deterministic simulations of AROME were available as guidance during the short-range forecast period for predicting potential severe weather for the night from 31 May to 1 June 2018 (Fig. 7). The first model run, initialised at 1200 UTC on 30 May, already hinted at the development of a major MCS over southwestern Germany and northeastern France (Fig. 7b), which moved to Belgium until 0600 UTC on 1 June. The spatio-temporal evolution of this simulated MCS coincided relatively well with the observed case (cf. Fig. 7b with 7a). AROME also simulated local-scale maximum hourly precipitation of 30 to 50 mm over the Greater Region during the passage of the MCS between 0000 and 0600 UTC on 1 June. The following run (30.05. 1800 UTC) suggested a similar scenario, although the precipitation pattern of the simulated MCS was slightly different (Fig. 7c). The subsequent 0000 UTC run on 31 May simulated once again a strong MCS (Fig. 7d), but the development was delayed by approximately two to four hours and the precipitation was forecast to be less intense over the Greater Region compared to the previous two runs. Then again, the solutions of the ensuing 0600 UTC and 1200 UTC runs were closer to the situations predicted by the two runs initialised on 30 May with regard to the spatio-temporal evolution of the MCS (cf. Figs. 7e,f with Figs. 7a-c). Overall, AROME consistently indicated the development of a major MCS over southwestern Germany and northeastern France which moved to Luxembourg and Belgium until the early morning of 1 June. However, the structure and the precipitation intensity of the MCS varied strongly between the model runs. Subjectively speaking, the AROME forecasts initialised at 1200 UTC and 1800 UTC on 30 May provided the best model guidance since the majority of the maximum hourly point rainfall measurements within the Greater Region ranged from 30 to 50 mm (the observation in Waldbillig being an exception).

By contrast, the probabilistic forecast issued from the ECMWF-EPS 0000 UTC run on 30 May and 31 May revealed a probability below 10 % for the occurrence of total precipitation exceeding 20 mm over Luxembourg between 31 May 1200 UTC and 1 June 1200 UTC (Fig. 8). Higher probability values were forecast in western and southern Germany (Fig. 8). Accordingly, the ECMWF's Extreme Forecast Index[3] did not hint at a potential extreme weather event in Luxembourg.

3 https://confluence.ecmwf.int/display/FUG/Extreme+Forecast+Index+-+EFI

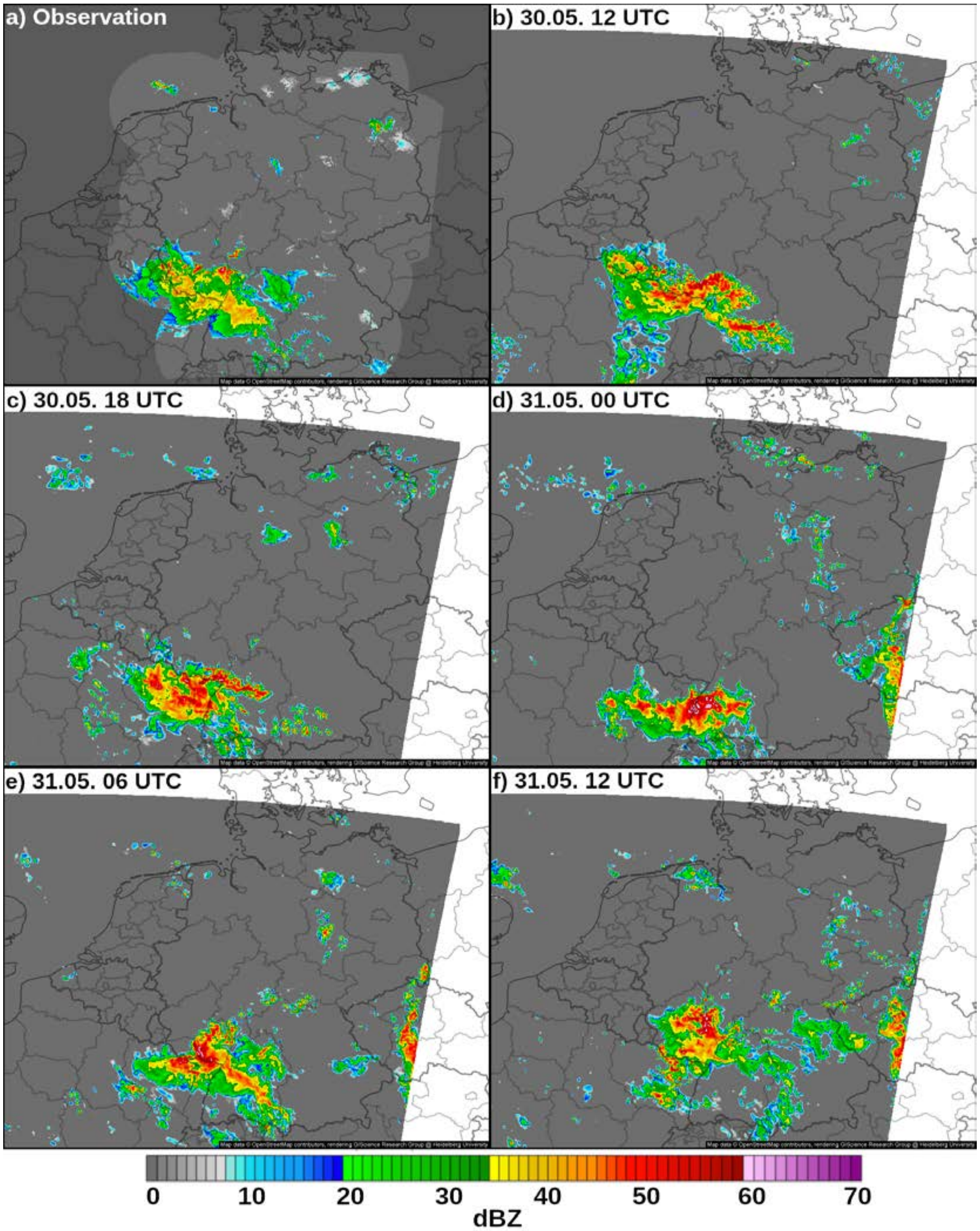

Figure 7: Comparison between the (a) observed and (b)-(f) simulated low-level radar reflectivity (dBZ) at 0000 UTC on 1 June 2018. Panel (a) shows the reflectivity measured by the C-band radar network of the DWD. Panels (b)-(f) show the low-level reflectivity simulated by AROME for different model initialisation times: (b) 30.05.2018 1200 UTC, (c) 1800 UTC, (d) 31.05.2018 0000 UTC, (e) 0600 UTC and (f) 1200 UTC. Sources: https://kachelmannwetter.com/de/radar-standard, https://kachelmannwetter.com/de/modellkarten/french-hd

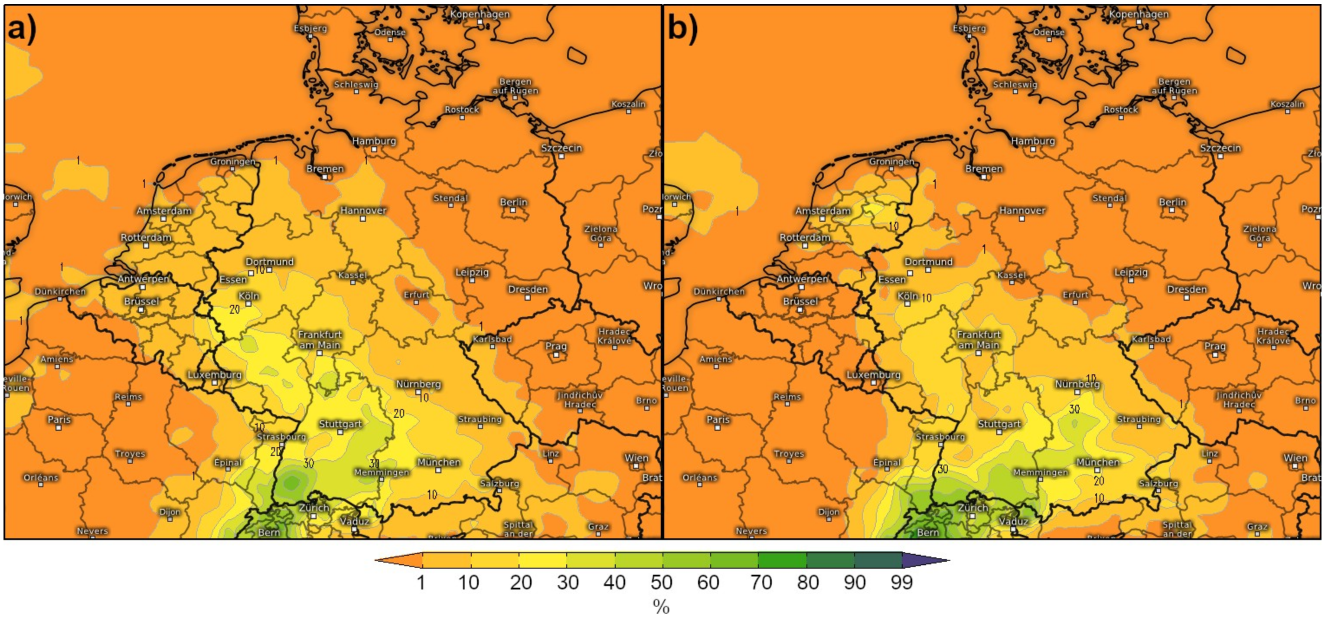

Figure 8: Event probability forecast valid for 1200 UTC on 1 June 2018 by the 0000 UTC run of ECMWF-EPS on (a) 30 May 2018 and (b) 31 May 2018 in terms of total precipitation exceeding 20 mm within the past 24 hours. Source: https://kachelmannwetter.com/de/modellkarten/euro

7. Summary and conclusions

The flash flood event in the Mullerthal region on 1 June 2018 was investigated with regard to the synoptic-scale and mesoscale meteorological context focusing on the atmospheric ingredients and predictability of this event. The MCS associated with the flood event developed in a weakly forced synoptic regime and the environment in the Greater Region was characterised by moderate latent instability (CAPE ranging from 500 to 1000 J kg^{-1}), weak lower-tropospheric flow, and moderate mid- to upper-tropospheric vertical wind shear. The mesoscale analysis showed that the torrential rainfall near Mullerthal was caused by a quasi-stationary deep convective cell, which formed downstream of the approaching MCS and was incorporated into the MCS later on. In comparison with the 22 July 2016 flash floods in the Vallée de l'Ermz studied by Pfister et al. (2018) and Mathias (2019), similarities were found among the strength of the decoupled tropospheric flow and the magnitude of the peak hourly precipitation amounts which initiated the floods.

The analysis of operational NWP model data revealed that the deterministic simulations of AROME captured the MCS relatively well, although there was significant forecast uncertainty regarding the precipitation structure and spatio-temporal evolution of the MCS. Furthermore, AROME indicated embedded point precipitation maxima with hourly accumulations of 30 to 50 mm, suggesting that there was at least some degree of predictability. On the contrary, a poor forecasting performance was diagnosed for the ECMWF-EPS. Hence, this case study highlights the need and usefulness of convection-resolving ensemble forecasts to improve the predictability of such low probability, high impact precipitation events in the future, which was also pointed out in several past studies (e.g., Vincendon et al. 2011, Evans et al. 2014, Golding et al. 2016).

Acknowledgements

The author thanks Alex Dewalque and Christophe Ferauge from the RMIB for providing radar data and Bram van't Veen for assistance with NLradar software. ECMWF's ERA5 reanalysis data is made available by the Copernicus Climate Change Service (https://cds.climate.copernicus.eu/). RADOLAN is accessible through DWD's open data data portal (https://opendata.dwd.de). The author also thanks the Kachelmann Group for archiving and visualizing operational NWP model data and making it freely available on its website (https://kachelmannwetter.com).

References

Bartels, H., Weigl, E., Reich, T., Lang, P., Wagner, A., Kohler, O., and Gerlach, N. (2004): Projekt RADOLAN, Routineverfahren zur Online-Aneichung der Radarniederschlagsdaten mit Hilfe von automatischen Bodenniederschlagsstationen (Ombrometer). DWD, Offenbach, Germany, 111 pp. [Available online: https://www.dwd.de/DE/leistungen/radolan/radolan_info/abschlussbericht_pdf]

Bechtold, P., N. Semane, P. Lopez, J.-P. Chaboureau, A. Beljaars, and Bormann, N. (2014): Representing equilibrium and non-equilibrium convection in large-scale models. *Journal of the Atmospheric Sciences*, **71**, 734-753. DOI: https://doi.org/10.1175/JAS-D-13-0163.1

Chen, Q., Fan, J., Hagos, S., Gustafson Jr., W. I., and Berg, L. K. (2015): Roles of wind shear at different vertical levels: Cloud system organization and properties. *Journal of Geophysical Research: Atmospheres*, **120**, 6551–6574. DOI: https://doi.org/10.1002/2015JD023253

Coniglio, M. C., Stensrud, D. J., and Wicker, L. J. (2006): Effects of Upper-Level Shear on the Structure and Maintenance of Strong Quasi-Linear Mesoscale Convective Systems. *Journal of the Atmospheric Sciences*, **63**, 1231–1252, DOI: https://doi.org/10.1175/JAS3681.1

Courtier, P., Freydier, C., Geleyn, J.-F., Rabier, F., and Rochas, M. (1991): The ARPEGE project at Météo-France, in: Workshop on numerical methods in atmospheric models. ECMWF, Reading, United Kingdom, 2, 193–232. [Available online: https://www.ecmwf.int/node/8798]

Evans, C., Van Dyke, D. F., and Lericos, T. (2014): How Do Forecasters Utilize Output from a Convection-Permitting Ensemble Forecast System? Case Study of a High-Impact Precipitation Event. *Weather and Forecasting*, **29**, 466–486. DOI: https://doi.org/10.1175/WAF-D-13-00064.1

Hersbach, H., Bell, B., Berrisford, P., Horányi, A., Muñoz Sabater, J., Nicolas, J., Radu, R., Schepers, D., Simmons, A., Soci, C., and Dee, D. (2019): Global reanalysis: goodbye ERA-Interim, hello ERA5. ECMWF Newsletter, No. 159, ECMWF, Reading, United Kingdom, 17-24. DOI: http://dx.doi.org/10.21957/vf291hehd7

Golding, B., Roberts, N., Leoncini, G., Mylne, K., and Swinbank, R. (2016): MOGREPS-UK Convection-Permitting Ensemble Products for Surface Water Flood Forecasting: Rationale and First Results. *Journal of Hydrometeorology*, **17**, 1383–1406. DOI: https://doi.org/10.1175/JHM-D-15-0083.1

Mathias, L. (2019): Synoptic-mesoscale analysis of the flash-flood-producing thunderstorm over the Vallée de l'Ernz on 22 July 2016. Administration de la Navigation Aérienne, MeteoLux, 18 pp. [Available online: https://www.meteolux.lu/fr/produits-et-services/publications/]

Seity, Y., Brousseau, P., Malardel, S., Hello, G., Bénard, P., Bouttier, F., Lac, C., and Masson, V. (2011): The AROME-France Convective-Scale Operational Model. *Monthly Weather Review*, **139**, 976–991. DOI: https://doi.org/10.1175/2010MWR3425.1

Pfister, L., Faber, O., Hostache, R., Iffly, J. F., Matgen, P., Minette, F., Trebs, I., Bastian, C., Göhlhausen, D., Meisch, C., and Patz, N. (2018): Crue éclair du 22 juillet 2016 dans la région de Larochette. Luxembourg Institute of Technology, Esch-sur-Alzette, Luxembourg, 16 pp.

Tiedtke, M. (1989): A comprehensive mass flux scheme for cumulus parameterization in large-scale models. *Monthly Weather Review*, **117**, 1779-1800. DOI: https://doi.org/10.1175/1520-0493(1989)117%3C1779:ACMFSF%3E2.0.CO;2

Vincendon, B., Ducrocq, V., Nuissier, O., and Vié, B. (2011): Perturbation of convection-permitting NWP forecasts for flash-flood ensemble forecasting. *Natural Hazards and Earth System Science*, **11**, 1529-1544. DOI: https://doi.org/10.5194/nhess-11-1529-2011

Appendix: media reports

Luxemburger Wort

- https://www.wort.lu/de/lokales/katastrophale-zustaende-nach-sintflutartigem-regen-5b10d747c1097cee25b8a5d4
- https://www.wort.lu/de/lokales/mit-dem-wasser-kommen-die-traenen-5b117f78c1097cee25b8a6fc

Tageblatt

- http://www.tageblatt.lu/digital/foto/ueberschwemmung-dramatische-bilder-aus-dem-muellerthal/
- http://www.tageblatt.lu/headlines/muellerthal-der-weg-zurueck-zur-normalitaet/
- http://www.tageblatt.lu/headlines/dreck-bruehe-verzweiflung-und-zusammenhalt-im-muellerthal/

Lëtzebuerger Journal

- https://www.journal.lu/top-navigation/article/sintflut-im-muellerthal/
- https://www.journal.lu/top-navigation/article/schaeden-in-millionen-hoehe/

RTL Lëtzebuerg

- https://www.rtl.lu/news/national/a/1188275.html
- https://www.rtl.lu/news/national/a/1190377.html